Influence of Ablation Impurities on Blunt Body Re-Entry Ionization

C. J. SCHEXNAYDER JR.* AND J. S. EVANS*
NASA Langley Research Center, Hampton, Va.

Electron density profiles which include the effect of ablated sodium impurity have been computed for the boundary layer on a blunt-nosed body re-entering the atmosphere at 7.62 km/sec (25,000 fps). Profiles are computed from the nose to a distance of four diameters along the RAM C-payload. A finite-difference, laminar, nonequilibrium chemistry boundary-layer program was used. Comparison of theory with S-band diagnostic antenna results, electron concentration deduced from X- and C-band attenuation data, and Langmuir probe data at several different aft body locations show that agreement is good at high altitude. At the lower altitudes there is disagreement between theory and S-band antenna data where the apparent discrepancy is attributed to the three body recombination rate constant used for deionization of sodium coupled with the effect of angle of attack.

Introduction

THE free electrons which are produced in hypersonic flowfield plasmas are the dominant factor in the entry radio blackout phenomenon. In order to define the blackout problem for a flight mission it is necessary to predict the magnitude and distribution of free electrons in the vicinity of the communication antennas. This involves analysis of complex systems of chemical and thermodynamic processes for the complete shock layer.[1] Also in the boundary layer, the ionization of impurities such as alkali atoms must be considered because of the presence of ablation products.[2] At low altitude, local equilibrium ionization of the alkali impurities is a good approximation to the truth, but finite-rate chemistry should be used when dealing with the problem at high altitude. Nonequilibrium boundary-layer calculations with alkali impurities have been done for flights involving slender bodies.[3-5] However, there are high altitude limits above which a thin boundary-layer approach is no longer valid. For the RAM vehicle this altitude is near 71 km (233,000 ft).[6] For altitudes of 71 km and above, viscous shock-layer calculations with nonequilibrium chemistry have been done[7] for analysis of RAM C flight results. These calculations do not include the effect of ablation impurities.

The purpose of this paper is to show the influence of an ablation impurity such as sodium on the blunt body re-entry ionization problem. A finite-difference, laminar, boundary-layer theory with ablation[8] was used that included a nonequilibrium chemical reaction scheme with 8 species and 15 reactions. The theoretical results are compared with results from three of the flight experiments onboard the RAM C payload in altitude range 36–71 km.

RAM C Flight Description

The RAM C payload was a 9° half-angle blunted cone with a nose diameter, d_N, of 30.5 cm and a length of 122 cm. The payload entered the atmosphere at a velocity of 7.62 km/sec (25,000 fps). Figure 1 gives the configuration and the trajectory information for all three flights. The RAM C-I flight[9] and the RAM C-III flight[10,11] were primarily material injection experiments, but each carried diagnostic instrumentation such as VHF telemetry antennas, X-band telemetry horns, a C-band beacon horn, and a Langmuir probe rake. For the C-III flight an S-band diagnostic antenna and a swept-bias electrostatic probe rake (4 probes) were added. The fixed-bias electrostatic probe rake (16 probes) for RAM C-III extended 14 cm into the flow, whereas in the C-I flight it extended only 7 cm into the flow. The location of the various diagnostic instruments used in the comparison of theory and experiment is given in Table 1, where x/d_N refers to axial distance from the nose. These two flights used Narmco

Table 1 Location of onboard rf and electrostatic probes

x/d_N	RAM C-I, C-III
2.3	S-band diagnostic antenna[a] (3348 MHz)
2.6	X-band telemetry horns (9210 MHz)
3.7	C-band beacon horn (5700 MHz)
4.0	Electrostatic probes

[a] On RAM C-III only

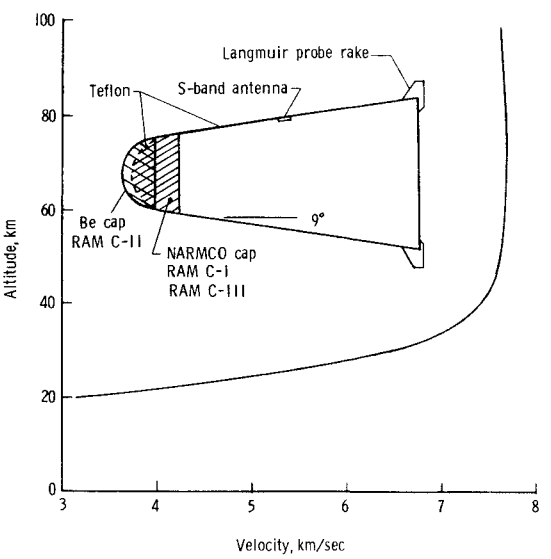

Fig. 1 RAM C configurations and entry profile.

Received February 20, 1973; revision received August 27, 1973.
Index categories: Thermochemistry and Chemical Kinetics; Reactive Flows.

* Aero-Space Technologist, Combustion Section, Hypersonic Vehicles Division.

Table 2 Reactions and rates used for calculations

	REACTION	Forward Rate Constant, k_f[a] A	B	C	Reverse Rate Constant, k_r[a] A	B	C	Third Body M
1.	$O_2 + M \rightleftarrows O + O + M$	3.6×10^{18}	-1.0	59400	3.0×10^{15}	-0.5	0	N, NO
2.	$O_2 + O_2 \rightleftarrows O + O + O_2$	3.3×10^{19}	-1.0	59400	2.7×10^{16}	-0.5	0	
3.	$O_2 + N_2 \rightleftarrows O + O + N_2$	7.2×10^{18}	-1.0	59400	6.0×10^{15}	-0.5	0	
4.	$O_2 + O \rightleftarrows O + O + O$	9.0×10^{19}	-1.0	59400	7.5×10^{16}	-0.5	0	
5.	$N_2 + M \rightleftarrows N + N + M$	1.9×10^{17}	-0.5	113100	1.1×10^{16}	-0.5	0	O_2, O, NO
6.	$N_2 + N \rightleftarrows N + N + N$	2.1×10^{22}	-1.5	113100	1.2×10^{21}	-1.5	0	
7.	$N_2 + N_2 \rightleftarrows N + N + N_2$	4.8×10^{17}	-0.5	113100	2.7×10^{16}	-0.5	0	
8.	$NO + M \rightleftarrows N + O + M$	4.0×10^{20}	-1.5	75600	1.0×10^{20}	-1.5	0	O_2, N_2
9.	$NO + M \rightleftarrows N + O + M$	7.9×10^{21}	-1.5	75600	2.0×10^{21}	-1.5	0	O, N, NO
10.	$NO + O \rightleftarrows O_2 + N$	3.2×10^{9}	1.0	19700	9.6×10^{11}	0.5	3600	
11.	$N_2 + O \rightleftarrows NO + N$	6.8×10^{13}	0	37500	1.5×10^{13}	0	0	
12.	$N + O \rightleftarrows NO^+ + e^-$	2.4×10^{10}	0.5	32400	4.0×10^{20}	-1.2	0	
13.	$Na + M \rightleftarrows Na^+ + e^- + M$	2.5×10^{11}	0.5	59670	6.0×10^{19}	-1.0	0	O, N, O_2, N_2
14.	$Na^+ + NO \rightleftarrows NO^+ + Na$	4.8×10^{10}	0.5	47710	1.0×10^{13}	0	0	
15.	$Na + e^- \rightleftarrows Na^+ + e^- + e^-$	3.7×10^{13}	0.5	59670	9.1×10^{21}	-1.0	0	

a. Form of rate constant is $k = AT^B \exp(-C/T)$ with k in cm^3/mole-sec or cm^6/$mole^2$-sec.

4028, a phenolic graphite charring ablator to protect the payload during re-entry. An analysis of the heat shield material showed that it contained at least 4700 ppm alkali by weight which was identified as being mainly sodium. The analysis was performed using emission spectroscopy with an uncertainty on the order of 10%. A previous analysis using a neutron activation technique gave similar results for sodium content within the 10% uncertainty. The RAM C-II flight[12] had a Be nose cap which was ejected at $\approx$56 km (184,000 ft), thereby exposing a teflon nose. The alkali content of the Be and teflon was negligible. All three payloads had teflon for heat protection on the afterbody ($x/d_N > 0.8$).

Theory

Inviscid flowfield properties were calculated using the streamtube method described in an earlier publication.[1] Boundary-layer properties for pure air and air with sodium were calculated using Blottner's program.[8] Changes made to adapt the Blottner program for our use were: 1) introduction of variable step size keyed to the magnitude of changes in chemical composition; 2) introduction of the species Na and Na^+ with corresponding additions to the reaction system; 3) replacement of the means for achieving conservation of elements; and 4) updating the chemical reaction rates.

Boundary-layer edge values of temperature, pressure, velocity, and species mass fraction were read from plots of inviscid profiles at a distance from the surface equal to the boundary-layer thickness, and the process was iterated until no change was obtained in boundary-layer thickness. Detailed information on the ablation rate and the distribution of ablation material in the boundary layer was given in a previous publication.[13] The wall boundary condition used was equilibrium composition with specified wall temperature. The 15 chemical reactions and the rates used in the program are given in Table 2. The species used are O_2, N_2, O, N, NO, NO^+, Na, and Na^+. Computations were carried out from an altitude of 30.6 km (100,500 ft) to 71.0 km (233,000 ft). The validity of carrying the boundary-layer calculations up to 71 km is discussed in Ref. 6. Vibrational and electronic degrees of freedom were assumed to remain in equilibrium with the translational degree of freedom. The electron temperature was assumed to be equal to gas temperature, which is a reasonable assumption in view of the experimental electron temperatures reported[7] for the RAM C-III flight.

Since NO^+ was the only ion in the Blottner air chemistry system while the inviscid flow chemistry included O^+, N^+, N_2^+, and O_2^+, it was sometimes necessary to specify the edge value of NO^+ concentration as equal to the sum of the inviscid flow values of NO^+, O^+, N^+, N_2^+, and O_2^+ concentrations. As was noted in an earlier publication,[1] a short chemistry system such as Blottner used gives nearly identical results to a long system at the aft body stations of the RAM C vehicle over the altitude range considered here (71 km and lower). Kang et al.[7] who emphasized the importance of using the long system at altitudes above 71 km for the RAM C flowfield analysis, also found that the long and short systems gave the same values of electron concentration at the aft stations for altitudes below 71 km. Both papers noted that the basic reason for validity of the short system was dominance of the NO^+ ion. Even though other ions may outnumber NO^+ in the production region at the nose, the charge rapidly transfers to NO^+ when the flow expands and cools. If charge transfer cannot take place (as, for example, at high altitudes because of the lowered collision rate) dominance of NO^+ at the rear stations will not occur unless it was also dominant in the production region.

No account was taken of the effect of teflon ablated from the afterbody heat shield ($x/d_N > 0.8$). The chief objective of the study was to evaluate the effect of finite-rate sodium ionization in a blunt body flowfield as compared to previous calculations in which equilibrium ionization of sodium was used. Finite-rate calculations in which both sodium and teflon ablation products were accounted for have been published,[5] but only the flow over a sharp cone was considered. For a sharp cone, the ionization of sodium and the attachment of electrons to pyrolysis products of teflon occur simultaneously in the boundary layer, but for the blunt RAM-C body the ions and electrons were principally generated on the nose cap, which was covered with Narmco. The question of whether a significant number of electrons are attached to teflon products at stations downstream of $x/d_N = 0.8$ is not answered in this paper, but two observations indicate that neglect of the effect of teflon ablation may be justified. One is that electron production in the nose region was completely

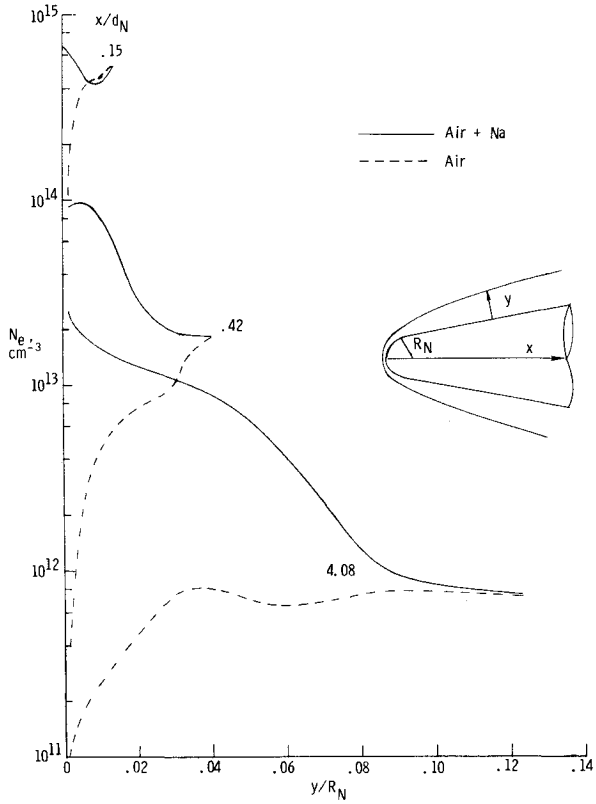

Fig. 2a Boundary-layer electron concentration profiles with and without ablation, altitude = 40.0 km.

independent of teflon ablation. The other is that, even for the sharp cone calculations,[5] the ratio of attached electrons to free electrons did not exceed 0.05. Some attachment of electrons might be expected near the cold wall but experimental evidence

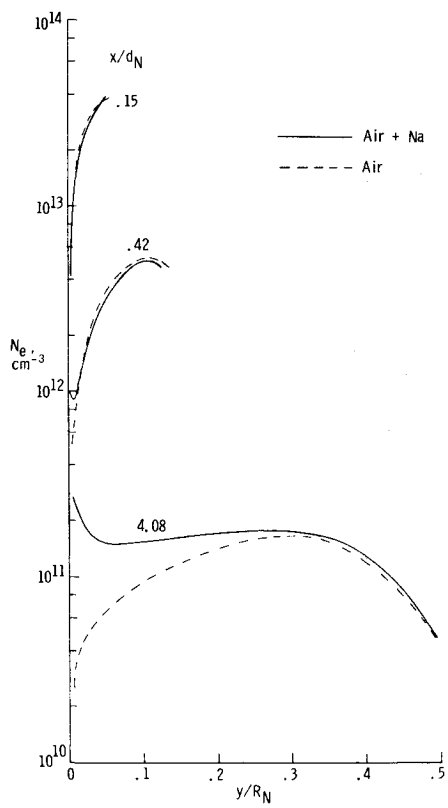

Fig. 2b Boundary-layer electron concentration profiles with and without ablation, altitude = 65.2 km.

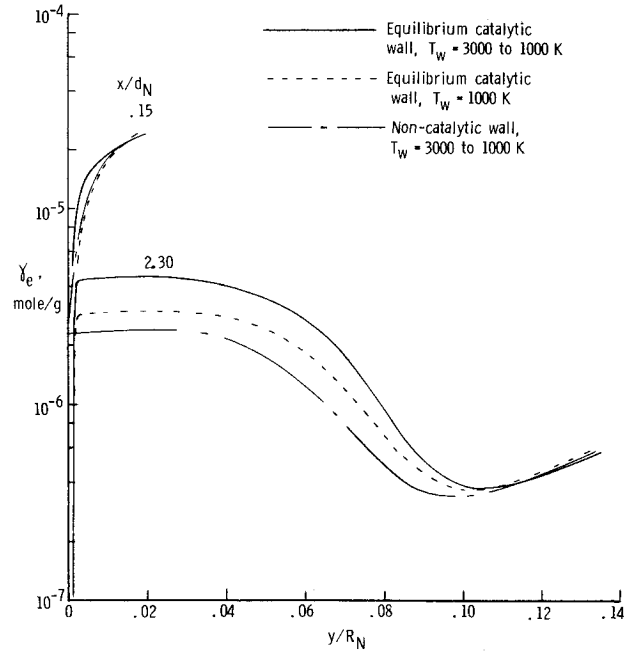

Fig. 3 Effect of wall conditions on boundary-layer electron concentration, altitude = 47.6 km.

by Starner[14] indicates that attachment in air$-C_2F_4$ mixtures is negligible at $T > 3000$ K. Reactions of the type $Na + O \leftrightarrows Na^+ + O^-$ were not included because they were found not to be the dominant source of ions in calculations[15] for a sharp cone at re-entry velocity of 6.83 km/sec (22,400 fps).

Discussion of Results

Typical calculated boundary-layer profiles are shown in Fig. 2. The pure air curves are included to illustrate the large effect of sodium ionization has on the boundary-layer values of N_e at 40.0 km (131,000 ft). The calculated increase is due to finite-rate ionization of sodium and is typical of results obtained in the altitude range 30–50 km. As shown in Fig. 2b sodium ionization does not greatly increase electron concentration at 65.2 km (214,000 ft). This is typical for altitudes from 60 km to the highest computed (71 km).

Theoretical profiles of the specific concentration of electrons (γ_e) are illustrated in Fig. 3. The γ_e curves are flat near the wall on the aft-portion of the body because the electrons cannot recombine with Na^+, the major ion. Because the density rises steeply near the wall an upturn in N_e profiles as shown in Figs. 2a and 2b is predicted.

Wall temperature varies from $T_w = 3000$ K at the stagnation point to a constant value of 1000 K downstream of the shoulder (with linear variation between), and very little difference was found between the computed γ_e profiles for this wall condition and those obtained with $T_w = 1000$ K at all points on the surface. A few calculations were made in which the equilibrium wall condition was replaced with a noncatalytic wall (all species). As Fig. 3 shows, this also had little effect on the γ_e profile peak.

In Fig. 4 peak values from profile curves (inviscid merged with boundary layer) are plotted as a function of altitude for two axial stations to show how sodium ionization in the boundary layer affects the peak N_e. Below 50 km, peaks of the pure air curves were in the inviscid flow; at higher altitudes they were in the boundary layer.[6,13] At $x/d_N = 0.15$ (45° location on spherical portion of nose) Na ionization does not greatly increase peak N_e. For $x/d_N = 2.3$ and other aft body stations the peak electron concentration below 60 km increased due to ionization of sodium. It is interesting to note that, in contrast with earlier equilibrium (for sodium only) results,[2] there is no rapid increase in N_e with increasing altitude for the air+Na curve ($x/d_N = 2.3$)

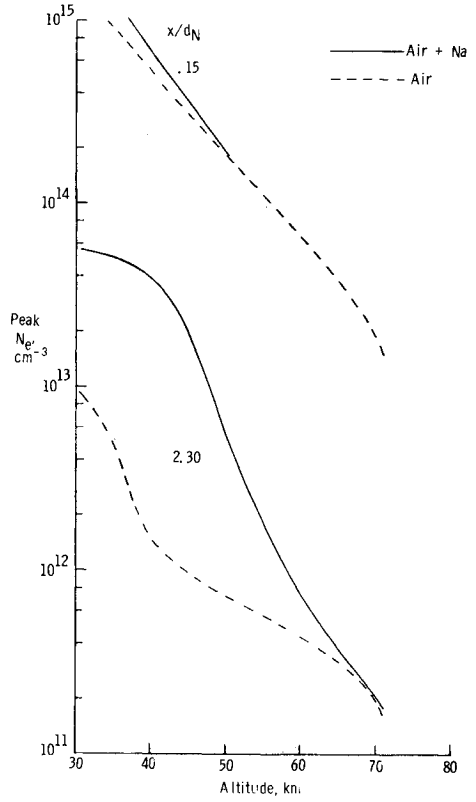

Fig. 4 Effect of sodium ionization on peak electron concentration.

beginning at 55 km (180,000 ft). This emphasizes the importance of making nonequilibrium calculations for Na ionization at these high altitudes.

Figure 5 illustrates the comparison of the flight data of RAM C-I and C-III (Langmuir probe data,[11,16] S-band diagnostic antenna admittance data,[10] and N_e inferred from signal attenuation at C and X-band frequencies[2,9,10]) with calculations of peak N_e (air + Na) at $x/d_N = 2.3$ and 4.08. As a result of excellent agreement between C-I and C-III Langmuir probe data only C-III Langmuir probe data are shown on this and subsequent figures. The comparison is good in the altitude range 55–71 km. At lower altitudes the S-band data indicates that peak electron concentration is lower than air + Na theory predicts by as much as a factor of 10. There is a greater degree of confidence placed on obtaining peak N_e values from the S-band antenna admittance data than the confidence level in obtaining N_e values from attenuation records for the RAM C-I flight. Since the comparison between S-band data and air + Na theory is poor in altitude region below 55 km the fault may lie with the Na + air theory and a method for improving the theory based on changes in Na ionization kinetics is presented later on.

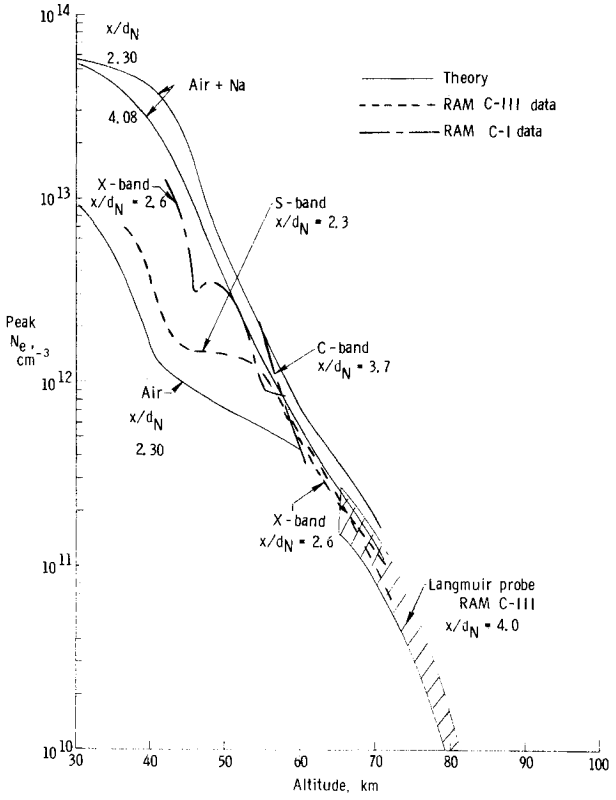

Fig. 5 Comparison of peak electron concentration with RAM C-I and C-III diagnostic data.

The pure air curve appears on Fig. 5 for reference and agrees well[6,13] with RAM C-II data[12] on the rear of the body (altitude range 37–55 km). Finite-rate ionization of Na is felt to be responsible for the difference between electron concentrations deduced from the RAM C-III data as compared to those from RAM C-II. Blackout and attenuation of X and C-band signals from the C-I[9] and C-III[10] flights occurred 6–8 km higher in altitude (3 sec earlier on attenuation records) than the corresponding data and reflectometer results from the RAM C-II flight.[12] This indicates that an additional source of electrons was present for the C-I and C-III flights in the altitude range 40–60 km.

In an attempt to explain the discrepancy between air and Na theory and data from the RAM C-III experiment, calculations to explore the effects of changing sodium reaction rates were done both at high altitude where there are experimental N_e profiles from Langmuir probe data[11,16] and at low altitude where the data from the S-band antenna[10] do not agree with theory. Figure 6 compares RAM C-III data with the results of changing the Na rates at a typical high altitude trajectory point (71.0 km).

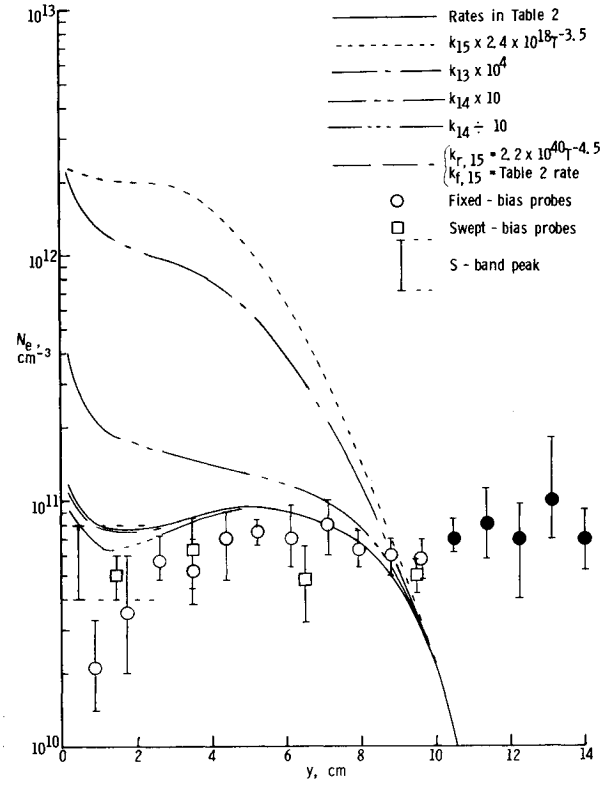

Fig. 6 Effect of changing sodium rates on electron concentration profile, altitude = 71.0 km, $x/d_N = 4$. (Filled symbols indicate heating effects described in Ref. 6. Top of S-band bar represents N_e at $x/d_N = 2.3$; low end of bar represents same peak value divided by 2 to adjust it to $x/d_N = 4$.)

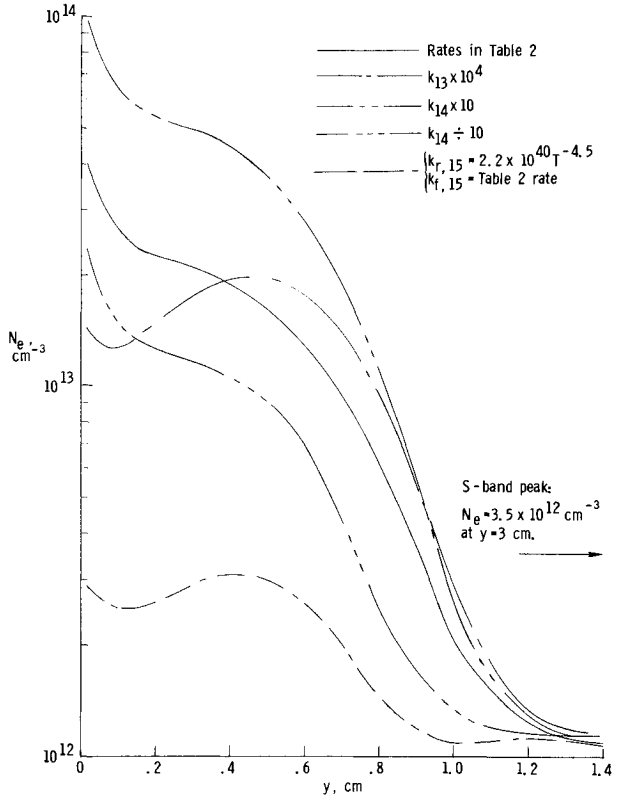

Fig. 7 Effect of changing sodium rates on electron concentration profile, altitude = 40.0 km, $x/d_N = 2.3$.

From the comparison it appears that the Na^+ production rates should not be increased over the values given in Table 2 since increases in the various production rate constants† only produce more electrons than were found in the RAM C-III experiment.‡ Slowing down the charge transfer rate constant ($\div 10$) lowers the theoretical N_e profile only slightly. One other change tried was to keep the production of Na^+ by electron impact slow (reaction 15 in Table 2) and at the same time increase the recombination rate constant to a value of $2.2 \times 10^{40} T^{-4.5}$. This change had no effect on the profiles at high altitude (>60 km), but did affect the low altitude profiles in a significant way, as will be discussed later.

The above mentioned comparison between theory and experiment indicates that the values for $k_{f,13}$, $k_{f,14}$, and $k_{f,15}$ in Table 2 are upper limit values and that caution should be exercised when using experimentally determined recombination rate constants to obtain forward endothermic rate constants. The fast recombination rate constants reported in the literature,[17,18] do not automatically imply that the corresponding forward rates are fast.

Figure 7 illustrates the effect of changing the Na reaction rate constants on the N_e profile at 40 km (typical for altitude range 30–50 km) for an aft body station ($x/d_N = 2.3$). Here again we see that increases in both forward and reverse rates do not help the theory to approach the peak N_e indicated by the S-band antenna experiment. An increase in the recombination rate constant ($Na^+ + e^- + e^- \rightarrow Na + e^-$) to $2.2 \times 10^{40} T^{-4.5}$, while keeping the opposite rate slow shows more promise of reducing the peaks than any of the other changes tried.§ Figure 8 shows the peak electron concentration plotted as a function of altitude with only this rate constant change (referred to as model II) compared to the experimental S-band results and the theory using the standard rates in Table 2. The comparison between model II and experiment is reasonably good for the entire altitude regime.

It is suggested that ionization of Na may not be a simple reaction characterized by a single forward rate constant for ionization but that it may be a more complex process[19] involving excited states. For example, the reaction mechanism

$$Na + M \underset{1}{\overset{2}{\leftrightarrows}} Na^* + M$$

$$Na^* + M \underset{3}{\overset{4}{\leftrightarrows}} Na^+ + e^- + M$$

involves 4 rates and 2 equilibrium constants. S-band antenna and Langmuir probe data from RAM C-III flight indicate that if the above mentioned mechanism does describe the ionization of sodium, reaction 4 is probably fast relative to the other rates, while the rate of formation of Na^+ ions is probably limited by the time required to produce Na*. Thus, the description of the ionization and recombination of sodium can be shortened to

$$Na + M \underset{1}{\overset{4}{\leftrightarrows}} Na^+ + e^- + M$$

so long as the equation is not used under conditions such that the forward and reverse rates are of comparable magnitude. Wilson[20] reported a similar approach for ionization of atoms (O and N) by electron impact; he assumed that the rate limiting step was excitation of the atoms. This method has also been used for rare gas atom ionization (see, for example, Ref. 21). The 3-body recombination rate constants were not discussed in those two

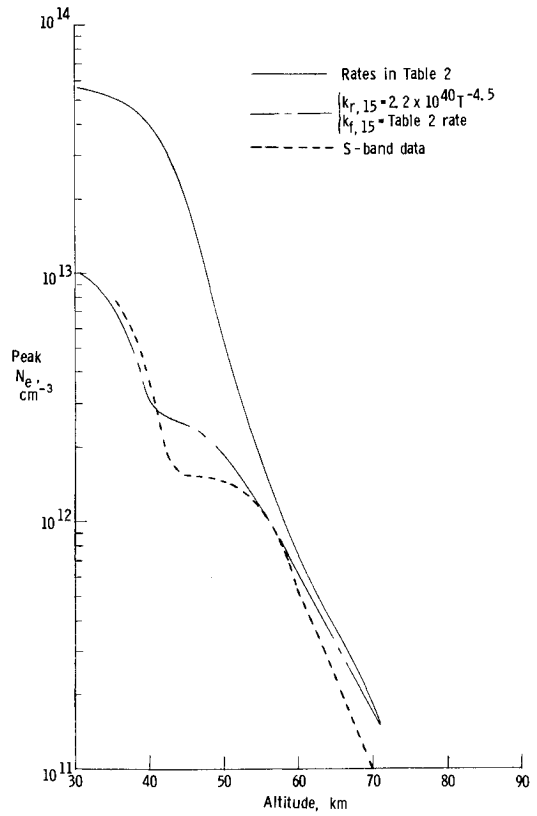

Fig. 8 Comparison of theoretical peak electron concentration with S-band diagnostic data from RAM C-III flight at $x/d_N = 2.3$.

† The rate constants for the following reactions were changed: 1) $Na + M \leftrightarrows Na^+ + e^- + M$ reaction using a recombination rate constant measured by Jensen,[17] 2) $Na + e^- \leftrightarrows Na^+ + e^- + e^-$ reaction with a recombination rate constant similar to the one measured by Dunn[18] for $C^+ + e^- + e^- \leftrightarrows C + e^-$ reaction, and 3) nominal change of 10 in the rate constant for charge transfer between NO^+ and Na. The forward rates were obtained through the relation $k_f = k_r K_{equil.}$

‡ Molecular weight of the ions in Langmuir probe data analysis[11] was 30, corresponding to the NO^+ ion. For Na^+ ions instead of NO^+, the N_e values would be about 13% lower.

§ No attempt was made to vary reaction 13 by the technique applied to reaction 15 but presumably this could reduce theoretical N_e's still further.

references. Recent results[22,23] indicate that ionization of alkali atoms in flames takes place from a state close to the ionization continuum by collision with an excited gas atom. Fowler and Preist[23] report that the actual collisional cross sections for alkali atom ionization are on the order of 10^{-16} cm^2 in flames. Kelly and Padley[24] have also reported cross sections for ionization of Na atoms in flames and discussed mechanisms for ionization.

The only remaining discrepancy is the assertion in Ref. 10 that peak N_e was 3.0 cm from the body at $x/d_N = 2.3$ in the altitude range 36–48 km. This would mean that the observed peak N_e is in the inviscid flow and not in the boundary layer. Because of the Na ionization all of the theoretical profiles in this altitude range have electron concentration peaks which lie in the boundary layer and are closer to the body than 3.0 cm.

A possible explanation can be seen by referring to Fig. 9. The solid line is the calculated N_e profile in the boundary layer. It can be seen that if the rates of Table 2 are used the highest value of N_e lies in the boundary layer and is due to sodium ionization. On the other hand, if the boundary-layer peak was much lower (as indicated by the other curve) then the peak in the inviscid region would be the highest point on the profile and would be appropriate for comparison with the peak position measured by the S-band antenna. Three calculated inviscid peaks[13] are shown in Fig. 9—one for each of three different values of the cone half-angle. The actual body flown was a 9° half-angle cone; calculations made for the other two angles were used to get approximate flowfields¶ for the body at angle of attack using an axisymmetric flowfield program. The re-entry body was spinning and was at angles of attack[25] of the order of 4° in this altitude range. Thus, the inviscid electron concentration peak at the antenna station cycled through shapes like those shown in Fig. 9, and it can be seen from the figure that once each cycle the height and position of the peak is approximately that called for by the S-band data analysis.

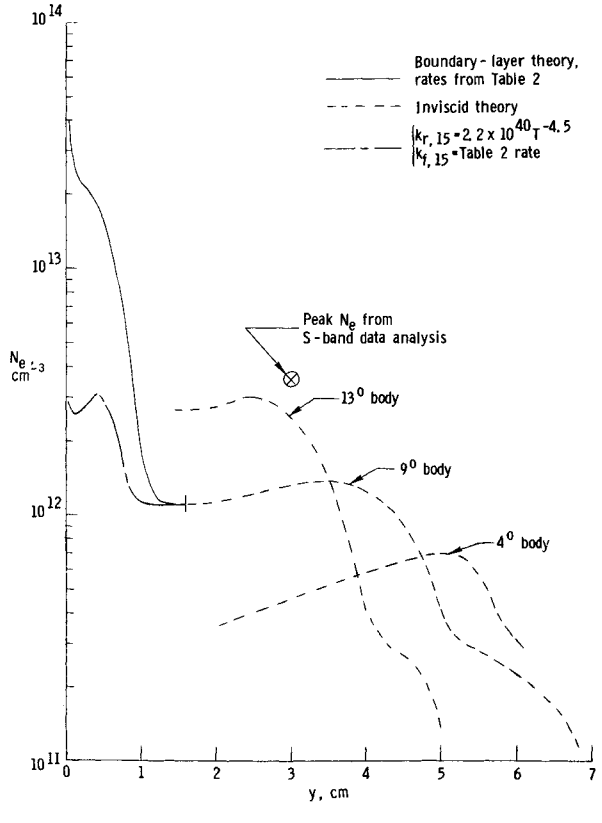

Fig. 9 Electron concentration profiles showing angle-of-attack effects in inviscid flow, altitude = 40 km, $x/d_N = 2.3$.

¶ Cross flow of electrons from windward to leeward side is negligible at the angles of attack considered and for this low altitude where boundary layer is thin.

It is interesting to note that around 36 km the S-band data analysis indicated a sharp change in measured distance to the peaks from 3.0–6.0 cm and that this increased distance of the peaks from the body surface persisted for the remainder of the data period for this antenna. Another analysis[25] which was concerned with body motions, reports that resonance of the pitch and roll motions occurred here and that the total wind angle went to 8.5°. It has also been reported[2] that transition from a laminar to a turbulent boundary layer may have occurred at about 32 km. These observations are simply noted here, no attempt is made to correlate them.

In the comparison made here uncertainty about the ionization rates for sodium is still a problem. One can see from Figs. 6–8 that the electron concentration is sensitive to the choice of rates. In particular N_e at low altitude at the rear of the body will depend on whether the 3-body recombination rate of Na^+ with electrons is fast enough for Na^+ to disappear in the flow time available. Since the rates and mechanisms for the production and disappearance of Na^+ are still uncertain (for example, when excited states of Na are considered[19]), there is a need for more experiments to obtain chemical kinetic data for application to the re-entry problem.

Conclusions

Electron density profiles which include the effect of ablated sodium impurity have been computed for the boundary layer on a blunt-nosed body re-entering the atmosphere at 7.62 km/sec (25,000 fps). A finite-difference, laminar, nonequilibrium chemistry boundary-layer program was used to compute profiles from the nose to a distance of four diameters along the RAM C payload. The results indicate that sodium ionization was the main contributor to electron concentration in the boundary layer at altitudes less than 60 km.

Comparison of the theoretical results with data from flight diagnostic instruments and with data deduced from signal attenuation measurements at several different aft body locations leads to the following conclusions: 1) There is good agreement between theory and experiment in the altitude range 55–71 km. 2) Finite-rate ionization of sodium is responsible for the difference in the values of N_e deduced from RAM C-I and C-III data as compared to data from the C-II flight. 3) Upper limits for some of the rate constants of the reactions for formation of sodium ions were deduced from the comparison between theory and data from the RAM C-III flight. 4) There is some disagreement between theory and S-band diagnostic antenna results in the altitude range 36–55 km.

The discrepancies are attributed to fast 3-body recombination ($Na^+ + e^- + e^- \leftrightarrows Na + e^-$) coupled with the effect of angle of attack. Since there is still uncertainty as to the appropriate mechanisms and rate constants for ionization of alkali atoms, further experimental work to obtain chemical kinetic data is desirable in the temperature range appropriate to the re-entry problems.

References

[1] Evans, J. S., Schexnayder, C. J., Jr., and Huber, P. W., "Computation of Ionization in Re-Entry Flowfields," *AIAA Journal*, Vol. 8, No. 6, June 1970, pp. 1082–1089.

[2] Huber, P. W., Evans, J. S., and Schexnayder, C. J., Jr., "Comparison of Theoretical and Flight-Measured Ionization in a Blunt Body Re-Entry Flowfield," *AIAA Journal*, Vol. 9, No. 6, June 1971, pp. 1154–1162.

[3] Kane, J. J., "Nonequilibrium Sodium Ionization in Laminar Boundary Layers," *AIAA Journal*, Vol. 2, No. 9, Sept. 1964, pp. 1651–1653.

[4] Lenard, M., "Ionization of Cesium and Sodium Contaminated Air in the Hypersonic Slender Body Boundary Layers," TIS-64S D22, Aug. 1964, General Electric Space Sciences Lab., King of Prussia, Pa.

[5] Braun, E. R., "Effects of a Fully Catalytic Wall on a Non-Equilibrium Boundary Layer Including Ablation Products," TIS-70S

D253, June 1970, General Electric Space Sciences Lab., King of Prussia, Pa.

[6] Evans, J. S., Schexnayder, C. J., Jr., and Huber, P. W., "Boundary Layer Electron Profiles for High-Altitude Entry of a Blunt Slender Body," *AIAA Journal*, Vol. 11, No. 10, Oct. 1973, pp. 1371–1372.

[7] Kang, S. W., Jones, W. L., Jr., and Dunn, M. G., "Theoretical and Measured Electron-Density Distributions at High Altitudes," *AIAA Journal*, Vol. 11, No. 2, Feb. 1973, pp. 141–149.

[8] Blottner, F. G., Johnson, M., and Ellis, M., "Chemically Reacting Viscous Flow Program for Multi-Component Gas Mixtures," SC-RR-70-754, Dec. 1971, Sandia Labs., Albuquerque, N. Mex.

[9] Akey, N. D. and Cross, A. E., "Radio Blackout Alleviation and Plasma Diagnostic Results from a 25,000 Foot Per Second Blunt-Body Re-Entry," TN D-5616, Feb. 1970, NASA.

[10] Schroeder, L. C., Swift, C. T., Akey, N. D., and Beck, F. B., "Material Injection Alleviations and Plasma Diagnostic Measurements During the RAM C-III Flight," AIAA Paper 72-690, Boston, Mass., 1972.

[11] Jones, W. L., Jr. and Cross, A. E., "Electrostatic Probe Measurements of Plasma Surrounding Three 25,000 Foot Per Second Re-Entry Flight Experiments," *The Entry Plasma Sheath and Its Effects on Space Vehicle Electromagnetic Systems*, Vol. I, NASA SP-252, 1971, pp. 109–136.

[12] Grantham, W. L., "Flight Results of a 25,000 Foot Per Second Re-Entry Experiment Using Microwave Reflectometers to Measure Plasma Electron Density and Stand-off Distance," TN D-6062, Dec. 1970, NASA.

[13] Schexnayder, C. J., Jr., Huber, P. W., and Evans, J. S., "Calculations of Electron Concentration for a Blunt Body at Orbital Speeds and Comparison with Experimental Data," TN D-6294, May 1971, NASA.

[14] Starner, K. E., "Evaluation of Electron Quench Additives in a Subsonic Air Arc Channel," *AIAA Journal*, Vol. 7, No. 12, Dec. 1969, pp. 2357–2358.

[15] Cresswell, J. et al., "Material Effects of Low Temperature Ablators on Hypersonic Wake Properties of Slender Bodies," TIS-67S-D255, May 1967, General Electric Space Sciences Lab., King of Prussia, Pa.

[16] Jones, W. L., Jr., "Probe Measurements of Electron Density Profiles During a Blunt-Body Re-Entry," Ph.D. thesis, June 1971, Dept. of Electrical Engineering, Virginia Polytechnic Institute and State University, Blacksburg, Va.

[17] Jensen, D. E. and Padley, P. J., "Kinetics of Ionization of Alkali Metals in H_2, O_2, N_2 Flames," *Transactions of the Faraday Society*, Vol. 62, No. 524, Aug. 1966, pp. 2140–2149.

[18] Dunn, M. G., "Measurement of $C^+ + e^- + e^-$ and $CO^+ + e^-$ Recombination in Carbon Monoxide Flows," *AIAA Journal*, Vol. 9, No. 11, Nov. 1971, pp. 2184–2191.

[19] "Effect of Contaminants on Observables in Re-Entry," AD 470984 (Contract DA-31-124-ARO-D-214), 1965, General Electric Space Science Lab., King of Prussia, Pa.

[20] Wilson, J., "Ionization Rate of Air Behind High-Speed Shock Waves," *Physics of Fluids*, Vol. 9, No. 10, Oct. 1966, pp. 1913–1921.

[21] McLaren, T. I. and Hobson, R. M., "Initial Ionization Rates and Collision Cross-Sections in Shock-Heated Argon," *Physics of Fluids*, Vol. 11, No. 10, Oct. 1968, pp. 2162–2172.

[22] Hollander, T., "Photometric Measurements on the Deviations from Equilibrium State in Flames," *AIAA Journal*, Vol. 6, No. 3, March 1968, pp. 385–393.

[23] Fowler, G. N. and Preist, T. W., "Ionization Cross Sections in Flames," *Journal of Chemical Physics*, Vol. 56, No. 4, Feb. 15, 1972, 1601–1605.

[24] Kelly, R. and Padley, P. J., "Measurement of Collisional Ionization Cross Sections for Metal Atoms in Flames," *Proceedings of the Royal Society of London*, Vol. 327A, No. 1570, April 4, 1972, pp. 345–366.

[25] Weaver, W. L. and Bowen, J. T., "Entry Trajectory, Entry Environment, and Analysis of Spacecraft Motion for the RAM C-III Flight Experiment," TM X-2562, June 1972, NASA.